Data Repository Item
ANALYTICAL DETAILS

FISSION-TRACK ANALYSIS

Apatite grains for fission-track analysis were separated from about 5 kg bulk samples using standard heavy liquids and magnetic separation techniques. Mounts were ground, polished and then etched with 5N HNO_3 at 20° C for 20 seconds to reveal the spontaneous tracks. The samples were then irradiated with thermal neutrons at the Radiation Center of the Oregon State University with a nominal neutron fluence of 9 x 10^{15} n cm^{-2}. The standard glass CN-5 was used as a dosimeter to measure the neutron fluence. After irradiation, induced fission tracks in the low-U muscovite that covered apatite grain mounts and glass dosimeter were etched in 40% HF at 20° C for 45 minutes. Apatite fission-track ages were measured and calculated using the external-detector and the zeta-calibration methods (Hurford and Green, 1983) with IUGS age standards (Hurford, 1990) and a value of 0.5 for the $4\pi/2\pi$ geometry correction factor. The observed grain-age distributions have been decomposed into different grain-age components by using the binomial peak-fitting method (Brandon, 1996; Stewart and Brandon, 2004). Tables DR1 and DR2 include apatite fission track data for the samples located in Fig. 1.

Sample	No. of crystals	Spontaneous		Induced		$P(\chi)^2$	Dosimeter		Age (Ma) ± 1σ
		ρ_s	N_s	ρ_i	N_i		ρ_d	N_d	
60a	17	0.42	27	2.67	1708	74.3	0.87	4126	2.5±0.5
60b	16	0.51	33	3.17	2053	99.5	0.91	4338	2.7±0.5
61	20	0.74	35	2.27	1072	95.5	0.88	4166	5.2±0.9
MAO	20	0.78	307	1.65	650	0.0	1.13	5360	86.9±11.8
35	20	0.12	18	0.34	511	78.4	1.15	5469	7.5±1.8
SAV1	20	0.37	33	1.36	1208	96.1	1.02	4835	5.1±0.9
31	25	0.39	15	2.16	827	86.8	1.14	5421	3.8±1.0
M1	25	0.38	31	2.08	1705	51.1	1.15	5445	3.9±1.3
36	26	0.18	17	0.75	713	78.1	1.14	5397	5.0±1.2
24	30	0.70	53	1.66	1254	79.1	1.18	7124	9.2±1.3
11	17	0.20	7	1.82	634	80.9	1.23	6150	2.5±0.9
5A1	20	1.26	57	2.41	1088	0.0	1.23	6150	10.1±4.9
5B2	11	0.11	3	1.08	288	39.1	1.23	6150	2.4±1.6
5E1	18	0.66	19	2.30	665	0.0	1.23	6150	4.3±2.4
5A2	20	0.49	18	1.81	1027	0.0	1.23	6150	6.1±2.3
IAS3	13	0.85	30	3.02	1064	85.4	1.07	5187	5.5±1.1

Table DR1. Central ages calculated using dosimeter glass CN5 and z-CN5=366.5±3.5. ρ_s: spontaneous track densities (x 10^5 cm^{-2}) measured in internal mineral surfaces; N_s: total number of spontaneous tracks; r_i and r_d: induced and dosimeter track densities (x 10^6 cm^{-2}) on external mica detectors (g=0.5); N_i and N_d: total numbers of tracks; $P(\chi^2)$: probability of obtaining χ^2-value for n degrees of freedom (where n=number of crystals-1); a probability >5% is indicative of an homogenous population. Samples with a probability <5% have been analyzed with the binomial peak-fitting method.

Sample	n	P1	P2
5A1	20	2.0±0.7 84.9%	76.0±12.6 15.1%
5A2	20	3.1±1.2 88.4%	31.8±12.9 11.6%
5E1	18	1.5±0.8 93%	35.7±10.5 7%
MAO	20	69.1±6.7 77.6%	181.9±23.6 22.4%

Table DR2. Apatite fission-track peak ages. n: total number of grains counted; binomial peak-fit ages (P1-P2) are given in Ma ± 1σ. Also given is the percentage of grains in a specific peak.

VITRINITE REFLECTANCE

Vitrinite is derived from the thermal degradation of wooden fragments of continental origin that can be dispersed in sediments (Stach et al., 1982; Teichmüller, 1987). Its reflectance strictly depends on the thermal evolution of the hosting sediments and is correlated to the stages of hydrocarbon generation and other thermal parameters in sedimentary environments (Durand, 1980; Scotti, 2003). Thus it is the most widely used parameter to calibrate basin modeling (Dow, 1977; Mukhopadhyay, 1994). The analysed samples were prepared according to standardized procedures described in Bustin et al. (1990). Random reflectance was measured under oil immersion with a Zeiss Axioplan microscope, in reflected monochromatic non-polarised light. On each sample, about twenty measurements were performed on vitrinite or bitumen unaltered fragments never smaller than 5 μm and only slightly fractured. Mean reflectance values (Ro for vitrinite and Rb for bitumen) were calculated from the arithmetic mean of these measurements. Rb values were converted into vitrinite equivalent reflectance data (Ro_{eq}) using Jacob's formula (Jacob and Hiltman, 1985). Table DR3 includes vitrinite reflectance data for the samples located in Fig. 1.

Tectonic domain	Stratigraphic age	Sample	Ro% ± 1σ	n° measurements
Apennine Platform	Miocene	33	0.37 ± 0.07	9
		10	0.56 ± 0.09	29
		29	0.40 ± 0.14	4
		34	0.43 ± 0.11	10
		35	0.36 ± 0.08	7
		35	0.34 ± 0.09	8
		18	0.25 ± 0.01	10
		14	0.39 ± 0.15	4
		15	0.55 ± 0.10	7
		19	0.36 ± 0.01	10
		21	0.38 ± 0.10	16
	Upper Triassic	7	0.60 ± 0.08 ‡	44
Lagonegro Basin	Lower Miocene	24	0.79 ± 0.08	29
		36	0.64 ± 0.13	19
		36	0.79 ± 0.17	9
	Lower-Mid Triassic	12	1.76 ± 0.33	24
		11	1.59 ± 0.15	15
		11	1.72 ± 0.11	26
Apulian Platform	Upper Miocene	5	1.54± 0.09	7
	Mesozoic	38	1.62 ± 0.06 ‡	30
Monte Croce Unit	Mid Miocene	60	0.76 ± 0.06	6
		61	0.59 ± 0.07	14

Table DR3. Vitrinite reflectance data. Sample location is shown in Fig. 1.
‡ Roeq data converted by using Jacob's formula (Jacob and Hiltman, 1985).

CLAY MINERALOGY

Each sample was prepared according to the procedures of Giampaolo and Lo Mastro (2000). X-ray powder diffraction analysis has been carried out with a Scintag Model X_1 Diffractometer (CuK_α radiation, solid state detector, spinner), according to the following steps:
- whole-rock samples (2÷70° $2\theta_{CuK\alpha}$, step size 0.05 °2θ, count time 3 s per step);
- glicolated 2÷16 μm grain-size fraction (1÷48° $2\theta_{CuK\alpha}$, step size 0.05 °2θ, count time 4 s per step);
- air-dried <2 μm grain-size fraction (1÷48° $2\theta_{CuK\alpha}$, step size 0.05 °2θ, count time 4 s per step);
- glycolated <2 μm grain-size fraction (1÷30° $2\theta_{CuK\alpha}$, step size 0.05 °2θ, count time 4 s per step).

This procedure was carried out in order to define the bulk-rock (Klug and Alexander, 1974; Rolli, 1992) and clay mineralogy with special regard to the content in mixed layers (Moore and Reynolds, 1989). The tube current and voltage were 40 mA and 45 kV, respectively.
X-ray oriented slides (<2 μm and 2÷16 μm grain-size fractions) were prepared by the pipette-on-slide method, keeping the specimen thickness as constant as possible, within the range of 1 to 3 mg

of clay per cm^2 of glass slide. The presence of expandable clays was determined for samples treated with ethylene glycol at 25°C for 15h. Diffraction peaks were analyzed using the X-ray system associated program by first removing a linear background level and then fitting them using a Pearson VII function.

FLUID INCLUSIONS

Fluid inclusions are small drops of fluid entrapped in crystals. Based on the time of trapping with respect to crystal growth, different types of fluid inclusions (primary, secondary, pseudosecondary) may occur in rock crystals (Roedder, 1984). The use of microthermometric analysis allows to obtain some quantitative information on: (i) homogenization temperatures (Th), which are indicative of the minimum trapping temperatures of the inclusions (Goldstein and Reynolds, 1994; Ceriani, 2003), and (ii) melting temperatures (Tm), which give information on fluid composition. By doing so, it is possible to choose the appropriate phase diagram for the examined fluid and to draw a P-T diagram by integrating fluid inclusion data with information obtained by other techniques (structural analysis, organic matter and clay mineralogy analyses, low temperature thermochronology). Limitations of this technique, particularly in sedimentary rocks, can derive from: (i) the small size of the inclusions (usually between 2 and 10 μm), and (ii) the possibility that the system was not closed (isoplethic) and/or isochoric (i.e. constant volume inclusions) since the time of entrapment. In the latter instance, fluid inclusions would record thermal re-equilibration at some stage of the tectonic evolution. This represents a common limitation for the study of carbonate rocks where non-isoplethic and non-isochoric conditions can develop more frequently for the presence of a 'soft' mineral such as calcite.

For the present study, in order to unravel the origin of the fluid inclusions, an accurate petrographic analysis was performed using 150 μm thick double polished wafers. For the veins associated with "brittle-ductile" shear zones and faults, the wafers were cut parallel to the XZ and XY planes of the strain ellipsoid (reconstructed by the geometry of conjugate structures; Ramsay and Huber, 1987).

Microthermometry was performed using a U.S.G.S. heating/freezing stage calibrated with synthetic fluid inclusions. Temperature of phase changes at $T \leq 0°C$ are accurate to ± 0.1°C; temperature ≥ 50°C are accurate to ± 1°C.

BURIAL AND THERMAL MODELING

Based on the data reported in Aldega et al. 2005 and Corrado et al. 2005, a simplified reconstruction of the burial and thermal history of representative sections was performed using the software package Basin Mod 1-D (Basin Mod® 1-D for WindowsTM, version 5.4 Software, 1996). Stratigraphic data such as thickness, lithologic composition, and age of formations are derived from regional studies (Scandone, 1972; Pescatore et al., 1999, and reference therein; Mazzoli et al., 2000, and reference therein). The main assumptions adopted for this reconstruction are that: (i) rock decompaction factors apply only to clastic units, according to the method of Sclater and Christie (1980), whereas carbonate units are not decompacted; (ii) seawater depth variations in time are irrelevant in modeling, because thermal evolution is mainly affected by sediment thickness rather than by water depth; (iii) thermal modeling has been performed using LLNL Easy %Ro method based on Burnham and Sweeney (1989) and Sweeney and Burnham (1990); (iv) thrusting can be considered instantaneous when compared with the duration of deposition of stratigraphic successions, as generally suggested by theoretical models (Endignoux and Wolf, 1990); (v) for the sake of simplicity, exhumation is considered linear within given time intervals; and (vi) a variable geothermal gradient has been adopted, with variable pre-thrusting values (see Aldega et al., 2005) and a syn-exhumation value of 45°C/km in case of fast exhumation rates (the latter estimate calculated according to Brandon et al., 1998).

Available measured indicators from clay mineralogy and organic matter studies constrained the experienced maximum burial. Apatite fission tracks data constrained the unloading path. Fluid inclusions data, when available, are located according to the timing and structural setting of the sampled vein systems.

AGE OF FOREDEEP SEDIMENTATION

The siliciclastic deposits that sit stratigraphically above the carbonate-dominated continental margin successions record tectonic loading and subsidence into the Apennine foredeep (e.g. Sgrosso, 1998; Patacca and Scandone, 2001). In Figure DR1, a regular progression of the onset of foredeep sedimentation may be observed for the main allochthonous units of the thrust belt (i.e., Apennine Platform and Lagonegro Basin), marking their progressive subsidence into the NE migrating foredeep in Middle Miocene times. A much younger – Messinian to Pliocene – onset of foredeep deposition is recorded from outcrop/subsurface units of the thrust belt belonging to the Apulian Platform domain.

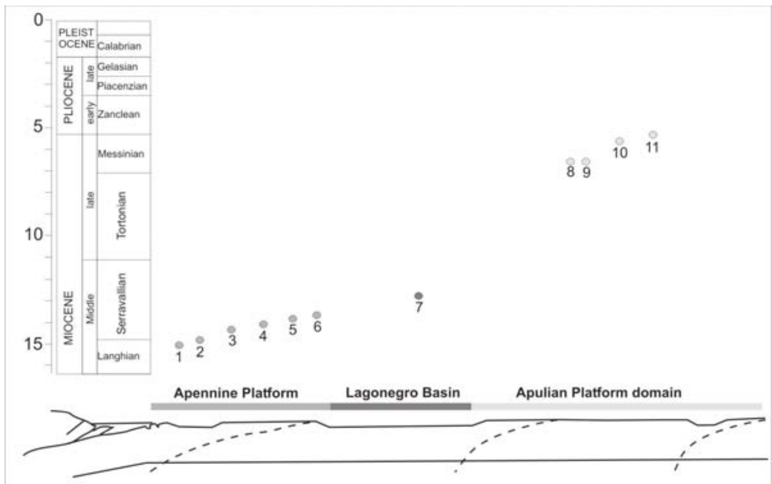

Fig. DR2. Diagram showing the onset of foredeep sedimentation at different sites in the southern Apennines (1: Monte Bulgheria; 2: Monte Cervati; 3: Sorrento; 4: Monti della Maddalena; 5,6: Monte Croce; 7: Serra Palazzo; 8,9: Monte Alpi; 10: Val d'Agri oil field; 11: Tempa Rossa oil field). Based on Sgrosso, (1998), including data from Patacca and Scandone (2001) and Shiner et al. (2004).

REFERENCES CITED

Aldega, L., Corrado, S., Di Leo, P., Giampaolo, C., Invernizzi, C., Martino, C., Mazzoli, S., Schiattarella, M., and Zattin, M., 2005, The Southern Apennines case history: thermal constraints and reconstruction of tectonic and sedimentary burials: Atti Ticinensi di Scienze della Terra - serie speciale, v. 10, p. 45-53.

Brandon, M.T., 1996, Probability density plot for fission-track grain-age samples: Radiation Measurements, v. 26, p. 663-676.

Brandon, M.T., Roden-Tice, M.K., and Garver, J.I., 1998, Late Cenozoic exhumation of the Cascadia accretionary wedge in the Olympic Mountains, northwest Washington State: Geological Society of America Bulletin, v. 110, p. 985-1009.

Burnham, A.K., and Sweeney, J.J., 1989, A chemical kinetic model of vitrinite maturation and reflectance: Geochimica Cosmochimica Acta, v. 53, p. 2649–2657.

Bustin, R.M., Barnes, M.A., and Barnes, W.C., 1990, Determining levels of organic diagenesis in sediments and fossil fuels, *in* McIleareath, I.A., and Morrow, D.W., eds., Diagenesis: Geoscience Canada Reprint, 4th series, p. 205-226.

Ceriani, A., 2003, Thermal constraints for fluid inclusions and applications to petroleum exploration: Atti Ticinensi di Scienze della Terra serie speciale, v. 9, p. 43-54.

Corrado, S., Aldega, L., Di Leo, P., Giampaolo, C., Invernizzi, C., Mazzoli, S., and Zattin, M., 2005, Thermal maturity of the axial zone of the southern Apennines fold-and thrust-belt (Italy) from multiple organic and inorganic indicators: Terra Nova, v. 17, p. 56-65, doi:10.1111/j.1365-3121.2004.00584.x.

Dow, W.G., 1977, Kerogen studies and geological interpretation: Journal of Geochemical Exploration, v. 7, p. 79-99.

Durand, B., 1980, Sedimentary organic matter and kerogen. Definition and quantitative importance of kerogen. in Durand, B., ed., Kerogen - Insoluble organic matter from sedimentary rocks. Ed. Tecnip. Paris, 13-33.

Endignoux, L., and Wolf, S., 1990, Thermal and kinematic evolution of thrust basins: a 2D numerical model, *in* Letouzey, J., ed., Petroleum Tectonics in mobile belts. Technip, Paris, 181-192.

Giampaolo, C., and Lo Mastro, S., 2000, Analisi quantitativa delle argille mediante diffrazione a raggi, in Fiore, S., ed., V Corso di Fomazione - Metodi di Analisi di Materiali Argillosi: Tito Scalo (PZ), Incontri scientifici - Istituto di Ricerca sulle Argille, v. 2, p. 109-146.

Goldstein, R.H., and Reynolds, T.J., 1994, Systematics of fluid inclusions in diagenetic minerals. SEMP Short Course 31, Tulsa, USA, p. 199.

Hurford, A.J., 1990, Standardization of fission track dating calibration: recommendation by the Fission Track Working Group of the I.U.G.S. Subcommission on Geochronology: Chemical Geology (Isotope Geoscience Section), v. 80, p. 171-178.

Hurford, A.J., and Green, P.F., 1983, The zeta age calibration of fission track dating: Isotope Geoscience, v. 1, p. 285-317.

Jacob, H., and Hiltmann, W., 1985, Disperse bitumen solids as an indicator for migration and maturity within the scope of prospecting for petroleum and natural gas - A model for NW Germany: DGMK, Forschungsbericht, v. 267, p. 1-54.

Mazzoli, S., Corrado, S., De Donatis, M., Scrocca, D., Butler, R.W.H., Di Bucci, D., Naso, G., Nicolai, C., and Zucconi, V., 2000, Time and space variability of “thin-skinned” and “thick-skinned” thrust tectonics in the Apennines (Italy): Rendiconti Lincei, Scienze Fisiche Naturali, 9 series, v. 11, p. 5-39.

Mukhopadhyay, P.K., 1994, Vitrinite reflectance as maturity parameter - petrographic and molecular characterization and its applications to basin modelling, in Mukhopadhyay P.K. and Dow, W.G., eds., Vitrinite reflectance as a maturity parameter: applications and limitations, p. 1-24.

Patacca, E., and Scandone, P., 2001, Late thrust propagation and sedimentary response in the thrust-belt–foredeep system of the Southern Apennines (Pliocene-Pleistocene), *in* Vai, G.B, and Martini, I.P., eds., Anatomy of an Orogen: the Apennines and Adjacent Mediterranean Basins: Kluwer Academic Publishers, p. 401-440.

Pescatore, T., Renda, P., Schiattarella, M., and Tramutoli, M., 1999, Stratigraphic and structural relationships between Meso-Cenozoic Lagonegro basin and coeval carbonate platforms in southern Apennines, Italy: Tectonophysics, v. 315, p. 269-286.

Roedder, E., 1984, Fluid Inclusions: Reviews in Mineralogy, v. 12, p. 646.

Scandone, P., 1972, Studi di geologia lucana: carta dei terreni della serie calcareo-silico-marnosa e note illustrative: Bollettino della Società dei Naturalisti in Napoli, v. 81, p. 225-300.

Sclater, J.G., and Christie, P.A.F., 1980, Continental stretching: an explanation of post-Mid Cretaceous subsidence on the Central North Sea Basin: Journal of Geophysical Research, v. 85, p. 3711-3739.

Scotti, P., 2003, Thermal constraints from the organic matter: Atti Ticinensi di Scienze della Terra, v. 9, Serie Speciale, p. 23-32.

Shiner, P., Beccacini, A., and Mazzoli, S., 2004, Thin-skinned versus thick-skinned structural models for Apulian Carbonate Reservoirs: constraints from the Val D'Agri Fields: Marine and Petroleum Geology, v. 21, p. .805-827.

Sgrosso, I., 1998, Possibile evoluzione cinematica miocenica nell'orogene centro-sud appenninico: Bollettino della Società Geologica Italiana, v. 117, p. 679-724.

Stach, E., Mackowsky, M.-Th., Teichmüller, M., Taylor, G.H., Chandra, D., Teichmüller, R., Murchinson, D.G., Taylor, G.H., and Zierke, F., 1982, Stach's Textbook of Coal Petrology: Berlin, Gebrüder Borntraeger, p. 535.

Stewart, R.I., and Brandon, M.T., 2004, Detrital-zircon fission-track ages for the ''Hoh Formation'': Implications for late Cenozoic evolution of the Cascadia subduction wedge: Geological Society of American Bullettin, v. 116, p. 60-75.

Sweeney, J.J., and Burnham, A.K., 1990, Evaluation of a simple model of vitrinite reflectance based on chemical kinetics: American Association of Petroleum Geologists Bullettin, 74, 1559-1570.

Teichmüller, M., 1987, Recent advances in coalification studies and their application to geology, *in* Coal and coal bearing strata: recent advances, *in* Scott, A.C., ed., Geological Society, London, Special Publication, v. 32, p. 127-169.